Physics Letters A 386 (2021) 126993

Contents lists available at ScienceDirect

Physics Letters A

www.elsevier.com/locate/pla

The effect of vacancy defects on the conductive properties of SiGe

Limeng Shen [a], Xi Zhang [a], Jiating Lu [a], Jiaqi Wang [b], Cheng Li [b], Gang Xiang [a,*]

[a] College of Physics, Sichuan University, Chengdu, 610064, China
[b] College of Physics, Xiamen University, Xiamen, 361005, China

ARTICLE INFO

Article history:
Received 19 June 2020
Received in revised form 26 October 2020
Accepted 30 October 2020
Available online 5 November 2020
Communicated by L. Ghivelder

Keywords:
SiGe
Vacancy defects
Formation energy
Electronic band
Conductive properties

ABSTRACT

Electronic band structures of defective silicon–germanium (SiGe) were described using *ab initio* calculations, and the influences of vacancy defects on the conductive properties of SiGe were studied. The analysis of formation energies of the defects indicates that a Si atom is easier to lose than a Ge one to form a single vacancy (SV) defect, and double vacancy (DV) defects might be more frequently found than two adjacent SV defects in SiGe. A vacancy could be formed more easily in Ge-rich than Si-rich SiGe. The band structures of SiGe compounds are affected conspicuously by defects, making most of the Si_xGe_{8-x} compounds with SVs show a trend to become to p-type, and almost all of the Si_xGe_{8-x} compounds with DVs turn to n-type. The p-type property might come from the vacancies with +2 charged state, and n-type property from the vacancies with −2 charged state.

1. Introduction

In recent decades, the semiconductor industry, especially the part based on the materials of group IV, is developing rapidly. Thereinto, two most important elementary substances silicon (Si) and germanium (Ge), both belonging to diamond lattice structures, are completely miscible with each other and can form silicon–germanium (SiGe) alloys as solid solutions with any proportion. SiGe alloys have attracted great attention due to several attractive properties, including adjustable band gaps [1–5] and enhanced carrier mobility [1,2] that could be exploited in many fields of application [6–9]. In addition, strained SiGe plays an important role in applications. For example, a host of devices is based on strained SiGe layers on Si substrates (so called "virtual substrates"), where lattice mismatch between SiGe and Si can bring strain and defects and engineer the properties of the devices [10–12].

Based on these facts, the study of defective SiGe deserves attention, since structural defects are unavoidable even in unintentionally doped unstrained SiGe according to thermodynamics [13–15]. Because of the existence of defects and impurities, previous experimental studies have found that most unintentionally doped epitaxial Si is n-type [16–18] and unintentionally doped epitaxial Ge is p-type [19–22]. However, unintentionally doped SiGe shows more complicated properties [16,23–27]: for instance, molecular beam deposited $Si_{1-x}Ge_x$ (x is 0.1, 0.25, 0.5, 0.75, and 1) samples show p-type [25], and SiGe single crystals grown by Czochralski technique are n-type when the content of Si is 0.01 [26]. In addition, experimental research has shown that heating treatment would affect the properties of SiGe alloys, including turning p-type to n-type [27], since the heating process influences the types and numbers of defects. Accordingly, recognition of the effect of defects and precise control of defects is essentially the key to design and fabricate SiGe-based devices with superior performance.

First-principles calculations of defects have become a cornerstone of research in semiconductors, even in novel two-dimensional (2D) semiconductors [28–31] and semiconductors with charged point defects [31–34], by providing insights into their fundamental physical properties. However, to the best of our knowledge, little theoretical work has been done to study the defects in SiGe systems with a range of elementary proportions, as well as the influences of the defects on the electronic and conductive properties.

In this work, we systematically studied several representative point defects in SiGe compounds, including single vacancy (SV) and double vacancy (DV) defects, these typical kinds of vacancy defects have been observed in experiments, especially in 2D materials [29,30], and did change the properties of materials. Using *ab initio* simulations, we investigated the formation energies of these defects and their influences on the properties of the SiGe compounds with different elementary proportions.

* Corresponding author.
E-mail address: gxiang@scu.edu.cn (G. Xiang).

https://doi.org/10.1016/j.physleta.2020.126993
0375-9601/

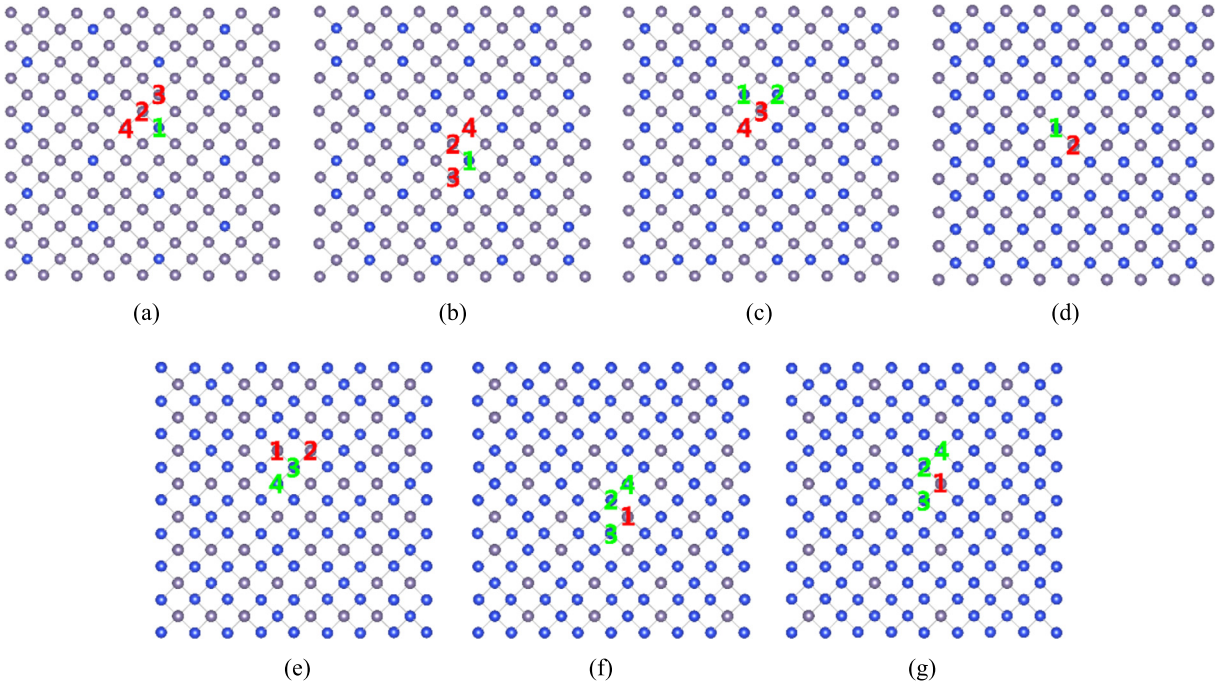

Fig. 1. Geometric structures of perfect Si_xGe_{8-x}, blue circles represent Si atoms and gray for Ge atoms, (a)–(g) is for $x = 1, 2, \ldots, 7$, as Si_1Ge_7, Si_2Ge_6, ...Si_7Ge_1, respectively. Various SV defects are labeled using defective positions in each Si_xGe_{8-x}, as for a tag of "1" in (a) is for $SV1_{17}$ defect in Si_1Ge_7. And the green (red) tag is for one Si (Ge) atom lost. (For interpretation of the colors in the figure(s), the reader is referred to the web version of this article.)

2. Calculation methods

Our first-principles calculations were performed using the Vienna *ab initio* simulation package (VASP) [35] based on density functional theory (DFT). We employed the plane-wave basis projector augmented wave (PAW) potentials [36] to describe the interaction between the valence electrons and the electrons in core region and generalized gradient approximation (GGA) of Perdew, Burke, and Ernzerhof (PBE) [37] for the exchange–correlation functions. The structure relaxations were carried out with a 600-eV plane wave cutoff, and throughout all calculations. The Brillouin zones (BZ) were sampled by a Γ-centred $2 \times 2 \times 8$ k-point meshes, during structural relaxation. All atoms were relaxed until the force criterion was less than 0.01 eV/Å and the energy differences were converged within 10^{-6} eV. For charged defects, the Coulomb interactions of an infinite periodic array of charged defects introduce a divergence. This divergence is usually removed by a uniform compensating charge ("jellium"), so called "jellium model", to maintain charge neutrality [32,34].

A large $4 \times 4 \times 1$ supercell (22.63 Å × 22.63 Å × 5.66 Å) of Si_xGe_{8-x} (with $x = 1$, 2, 3, 4, 5, 6 and 7) was built to investigate the effect of various defects in SiGe compounds. All the possible symmetrical structures for Si_xGe_{8-x} have been optimized (shown in Fig. 1 in supplementary material), and the energetically favored structures have been selected for subsequent studies. Then various kinds of SV defects were put into these optimized SiGe structures, with the principle that defects should be distributed uniformly and symmetrically. DV defects were brought into all these SiGe structures by choosing two nearest adjacent atoms and knocking them off, following the principle mentioned above.

To characterize the thermodynamic stabilities of these defects in SiGe and compare the formation probabilities with each other, we employed the formation energy of a defect D in charge state q, defined as [32,38]:

$$\Delta H_f(D, q, E_F) = E(D, q) - E_{\text{tot(pristine)}} + \sum_i n_i \mu_i + q(E_{\text{VBM}} + E_F)$$

where $E(D, q)$ and $E_{\text{tot(pristine)}}$ represent the total energy of the Si_xGe_{8-x} supercell with and without defects, respectively, n_i is the number of the removed Si atoms or Ge atoms in corresponding defective Si_xGe_{8-x}, and μ_i is the chemical potential of one Si atom or Ge atom in its pristine crystal cell, and defined as $\mu_i = E_{\text{Si(Ge)pristine}}/n_{\text{Si(Ge)}}$, where $E_{\text{Si(Ge)pristine}}$ and $n_{\text{Si(Ge)}}$ represent the total energy of pristine crystal cell and the number of the atoms in it, respectively. And, E_F is the Fermi level with respect to E_{VBM} the valence-band maximum (VBM) of the pristine material E_{VBM}.

3. Results and discussion

Fig. 1 shows the optimized energetically favored structures of Si_xGe_{8-x}, with x ranging from 1 to 7, respectively. Considering the fact that a small concentration incorporation of dopants or defects can result in several orders of magnitude decrease of electrical resistivity in IV semiconductors (for instance, 10^{-4}% doping of phosphorous atom in Si causes 7 orders of magnitude decrease of resistivity [39,40]), the defect concentration in our computational study on SiGe compounds might be too large. In fact, we used as big a supercell with 128 atoms as we can afford based on our computational capability to do the calculations, which results in a concentration of defects of about 1%, still much bigger than that of defects (not more than 10^{-7}% [41,42]) in real unintentionally doped SiGe samples. Therefore, instead of trying to get the absolute level of Fermi energy, we mainly focus the formation energy of the defects and the movement of the Fermi level induced by the defects to explore the influence of the defects on the conductive properties of SiGe.

The SV defects in SiGe were presented in Fig. 1. The tag "1" in Fig. 1(a) represents that on position "1" in Si_1Ge_7 there is a Si vacancy, which is named as $SV1_{17}$. Since there are four equivalent nearest Ge atoms around position "1", we have chosen one of the four sites, for instance, position "2", and name the Ge vacancy on position "2" as $SV2_{17}$. $SV3_{17}$ and $SV4_{17}$ are the two different Ge vacancies at the second nearest sites. The other defects in Si_xGe_{8-x}

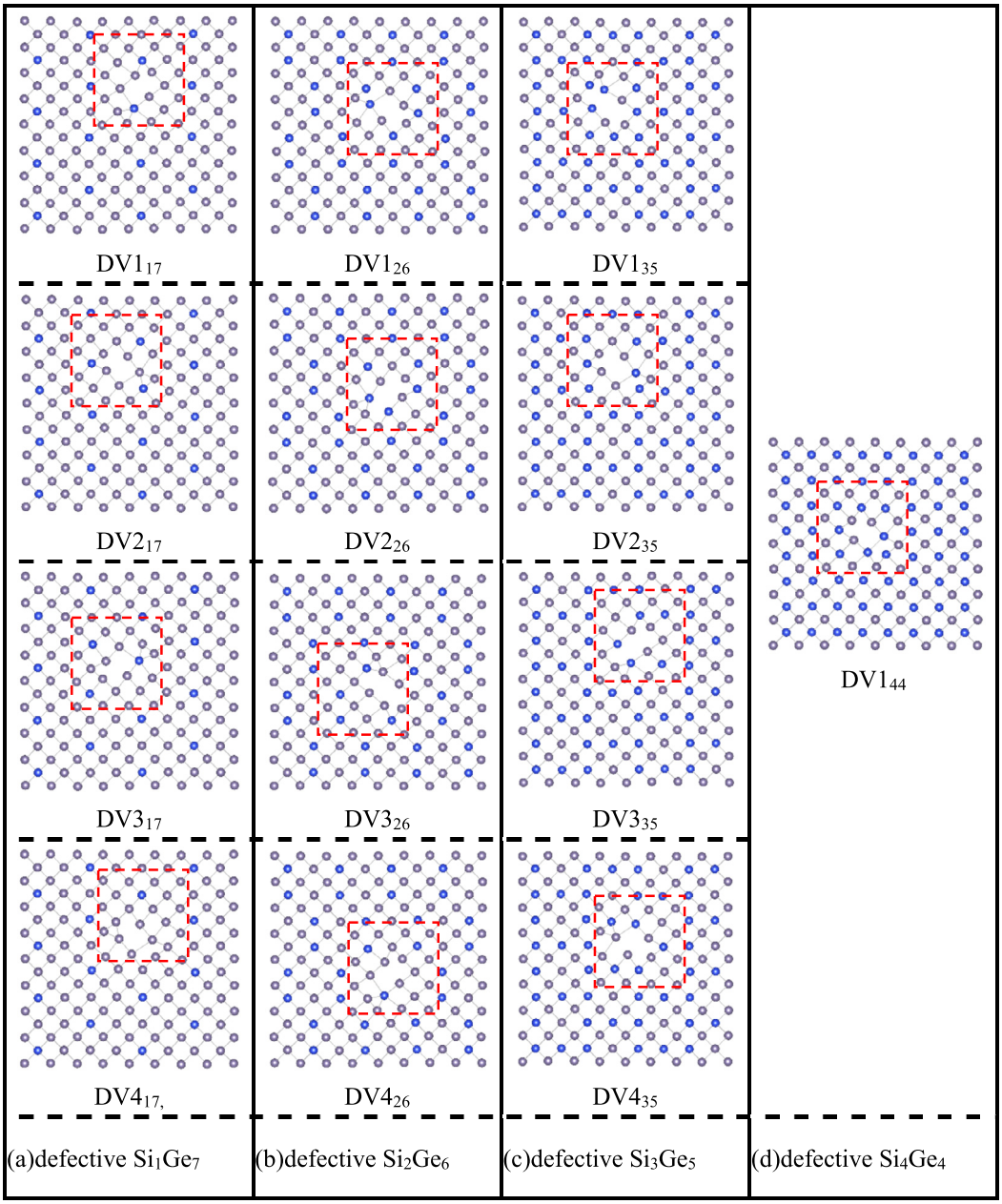

Fig. 2. Optimized structures of typical DV defects in (a) Si_1Ge_7, (b) Si_2Ge_6, (c) Si_3Ge_5, and (d) Si_4Ge_4. For clearer observation, all the defect areas are surrounded by red dotted lines in each atomic diagram of DV defective Si_xGe_{8-x} supercell.

compounds were labeled in this way as well, and the green (red) tag is for one Si (Ge) atom lost. All possible sites of SV defects were selected, and others are equivalent to these in infinite periodic array, respectively.

Typical DV defects, including those in Si_1Ge_7, Si_2Ge_6, Si_3Ge_5, and Si_4Ge_4 were shown in Fig. 2. The structures of DV defects in Si_7Ge_1, Si_6Ge_2 and Si_5Ge_3 are nearly same as Si_1Ge_7, Si_2Ge_6 and Si_3Ge_5, respectively, except that Si and Ge atoms exchange their sites. It is noted that there are four types DV defects in Si_1Ge_7, Si_2Ge_6, and Si_3Ge_5, respectively, while there is only one type DV defect in Si_4Ge_4, in consideration of the symmetry.

The formation energies for all these neutral vacancy defects in Si_xGe_{8-x} supercells were calculated and plotted in Fig. 3. As shown in Fig. 3(a), the formation energies of neutral SV defects are distributed in 1.75–3.66 eV, where the most formation energy of a Si SV defect is lower than a Ge SV defect, which implies that it is easier for Si atom to lose in SiGe systems. And the formation energies of SV defects increase as the silicon fraction x increases in Si_xGe_{8-x}, which is consistent with the results reported by J. Vanhellemont et al. that a vacancy could be formed more easily in pure Ge than in pure Si [43].

The formation energies of neutral DV defects are between 2.10 eV and 4.28 eV, shown in Fig. 3(b). Apparently, a DV defect is more energetically favored than two SV defects added together. For example, a $DV4_{17}$ defect in the Si_1Ge_7 supercell with the formation energy of 2.10 eV, would aggregate from one $SV1_{17}$ defect and $SV2_{17}$, owing to the total formation energy of these two SV defects ($1.75+2.02=3.77$ eV) is much higher than that of the $DV4_{17}$ defect. It indicates a higher appearance frequency of DV defects in our SiGe systems than that of two adjacent SV defects. Besides, a similar linear relationship between the vacancy formation energy and the concentration x of Si in Si_xGe_{8-x} was also observed. The formation energies of DV defects with one Si atom and one Ge atom lost are lower than that with two Ge atoms lost in Ge-rich

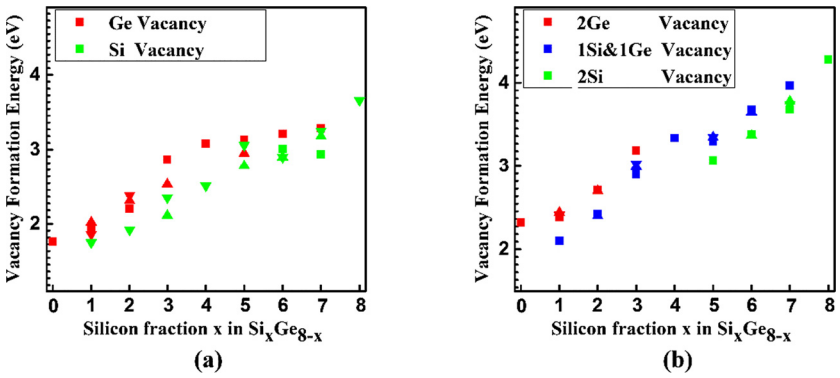

Fig. 3. Comparison results of vacancy formation energies (E_f (eV)) of various types of SV and DV defects in Si_xGe_{8-x} supercell. Besides, formation energies of SV and DV defects in pure Si ($x = 1$) and Ge ($x = 0$) are also shown. The red dots are for the Ge vacancy defects, green for the Si vacancy defects, and blue for the DV defects that with one Si and one Ge atom lost, different shapes are for all the possible types of vacancy defects mentioned before.

Table 1
The Fermi energies (E_F) and band gaps (E_g) calculated by PBE and HSE approximations, and their difference values (Δ) in pristine Si_xGe_{8-x}.

	Ge	Si_1Ge_7	Si_2Ge_6	Si_3Ge_5	Si_4Ge_4	Si_5Ge_3	Si_6Ge_2	Si_7Ge_7	Si
PBE					$4 \times 4 \times 1$ **supercell**				
E_F (eV)	3.78	4.04	4.28	4.57	4.81	5.09	5.29	5.88	5.93
E_g (eV)	0.06	0.24	0.40	0.42	0.55	0.46	0.48	0.45	0.66
PBE					$1 \times 1 \times 1$ **supercell**				
E_F (eV)	3.85	4.02	4.34	4.54	4.80	5.05	5.37	5.61	5.88
E_g (eV)	0.06	0.25	0.29	0.39	0.55	0.46	0.30	0.35	0.67
HSE06									
E_F (eV)	3.45	3.69	3.95	4.19	4.46	4.71	4.99	5.24	5.51
E_g (eV)	0.71	0.87	0.93	1.03	1.10	1.03	0.87	0.92	1.14
HSE06−PBE									
ΔE_F (eV)	−0.40	−0.34	−0.38	−0.35	−0.33	−0.34	−0.38	−0.37	−0.37
ΔE_g (eV)	0.65	0.62	0.64	0.64	0.55	0.57	0.57	0.57	0.47

Si_xGe_{8-x}, while two Si atoms vacancies would appear more easily in Si-rich Si_xGe_{8-x}, because Si atoms tend to lose more easily in SiGe systems, as mentioned before.

The band structures of pristine Si_xGe_{8-x} compounds were shown in Fig. 4. The resulting band structures of Si_xGe_{8-x} are similar to those of Si and Ge, which almost have an indirect band gap about 0.24–0.55 eV, shows that the VBM is at Γ point and closer to the E_F than the conduction band minimum (CBM). The band gaps are smaller than that in practical Si and Ge, since DFT calculation might underestimate the band gap in Si and Ge [44,45]. The more precise approach might be based on evaluation of the electron self-energy operator within the GW approximation [44], which in terms of the dynamically screened Coulomb interaction (W) and the dressed Green's function (G); or use hybrid HSE06 [45,46] exchange-correlation functional that mixes the PBE exchange part with 37.5% of Hartree-Fock exchange in the short range to match the experiment band gap. However, these methods are too time-consuming for our defective supercells. Since our main objective is to study the influences of vacancy defects on the conductive properties of SiGe, we focus mainly on analyzing the trend of the band variation and the movement of the Fermi level. Nevertheless, we also employed a smaller $1 \times 1 \times 1$ supercell (5.66 Å × 5.66 Å × 5.66 Å) with 8 atoms to compare the simulated results calculated by PBE and HSE approximations. The Fermi energies (E_F) and the band gaps (E_g) of pristine Si_xGe_{8-x} calculated by PBE and HSE approximations were shown in the Table 1. It can be seen that, E_F values calculated by PBE approximation are overestimated by 0.33 eV–0.38 eV, while E_g values calculated by PBE approximation are underestimated by 0.55 eV–0.64 eV with respect to the corresponding values calculated by HSE approximation.

As a typical example, Fig. 5 shows the band structures of Si_1Ge_7 compounds with different SV and DV defects. Obviously, the band structures of defective Si_1Ge_7 compounds have a distinct variation compared with that of pristine Si_1Ge_7 compound, owing to the existence of defects. The Fermi levels of all Si_1Ge_7 compounds with SV defects shift down obviously, indicting the incorporation of SV defects would enhance the p-type conductive properties. Although the Fermi levels eventually get into the valence band and indicate a metallic property owing to the much higher centration of defects we investigated than experimental ones as mentioned before, the analysis of the Fermi level shifting could still throw light upon the influences of vacancy defects on the conductive properties of SiGe compounds. On the other hand, most of the Si_1Ge_7 compounds with DV defects change to n-type, owing to the band gap narrowing and Fermi level shifting toward the CBM.

To further understand the electronic and conductive properties of all the considered defective Si_xGe_{8-x} compounds, we employed density of states (DOS) calculation, which were shown in Fig. 6. The shapes of the total DOS for the pristine Si_xGe_{8-x} compounds are almost similar, and cohere with their band structures. The band gaps (E_g) of them increase gradually from 0.24 eV to 0.55 eV as x increases. This variation agrees with the experiments and other more accurate calculation methods [1]. The E_g we calculated is smaller than experimental results, since DFT calculation usually underestimates the band gap in Si and Ge. It is observed that the total DOS of most SV defective Si_xGe_{8-x} (except Si_7Ge_1) shift up slightly, after all the E_F are normalized to zero, as shown in Fig. 6(a)–(f) upper; And the zero DOS positions of them shift up from the VBM to nearly the CBM (relative to their pristine structures), which is resulted from defective energy levels. These details mean that the E_F of these SV defective Si_xGe_{8-x} shift down, showing p-type property. Whereas, the E_F of SV or DV defective Si_7Ge_1

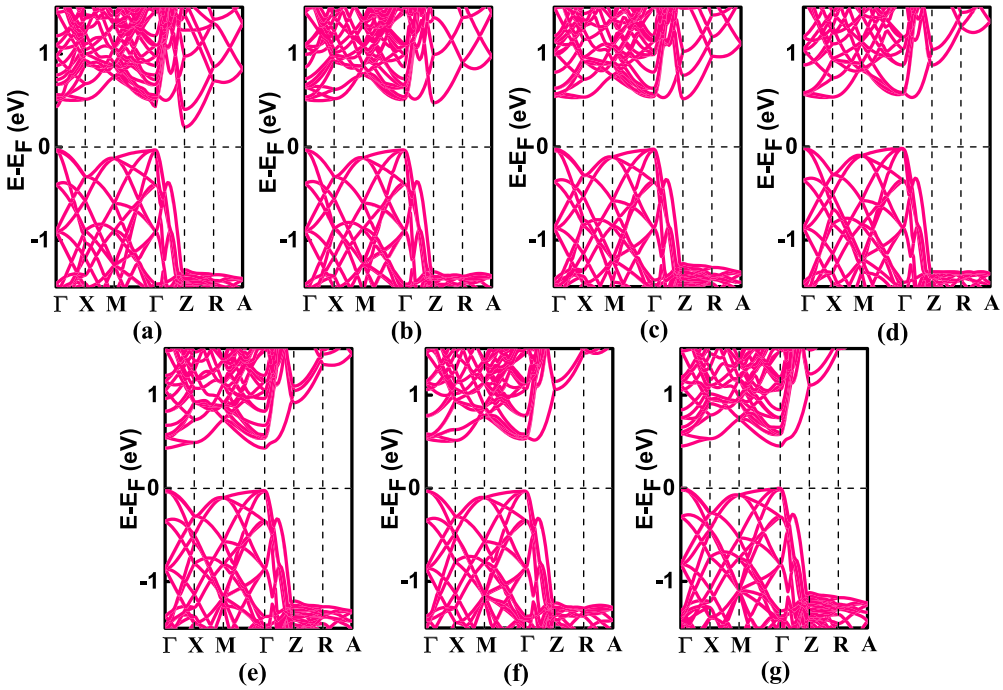

Fig. 4. Electronic band structures of pristine Si_xGe_{8-x} compounds, (a)–(g) is presented for Si_1Ge_7, Si_2Ge_6, ..., Si_7Ge_1, respectively.

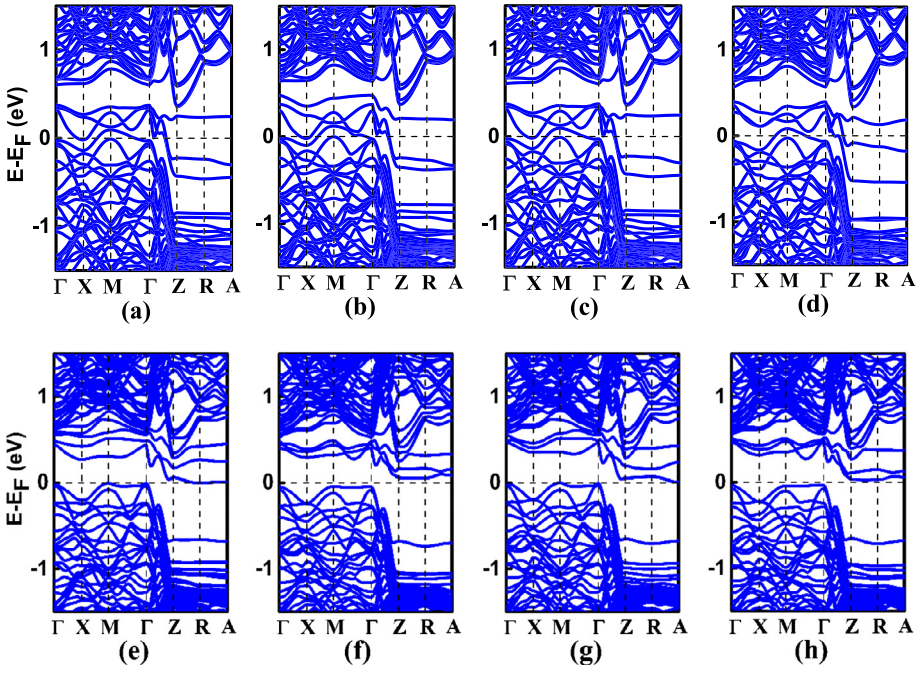

Fig. 5. Electronic band structures of Si_1Ge_7 with various kinds of SV and DV defects: (a)–(d) is for $SV1_{17}$, $SV2_{17}$, $SV3_{17}$, and $SV4_{17}$; (e)–(h) is for $DV1_{17}$, $DV2_{17}$, $DV3_{17}$, and $DV4_{17}$.

shift up, which can be seen in Fig. 6(g), exhibiting n-type property. Besides, as for the other DV defective Si_xGe_{8-x}, the total DOS and the zero DOS positions don't shift, as shown in Fig. 6(a)–(f) under. Then, there are some energy levels going deep into the CBM versus pristine structures, resulting in the electrons going into conductive bands more easily, leading to n-type property.

Moreover, the formation energies of the different charge states of the vacancy as a function of Fermi energy E_F, throw light upon the sources of the different conductive properties, as shown in Fig. 7. There are four permitted charge states for a vacancy in SiGe, ranging from (-2) to $(+2)$ [47]. The defect $SV1_{17}$ shows p-type property as previously mentioned, which might come from +2 charge state vacancy ($SV1_{17}{}^{+2}$), because of its lowest formation energy at VBM, as shown in Fig. 7 (a). Similarly, because of the lowest formation energies at CBM, $DV4_{17}{}^{-2}$, $SV3_{71}{}^{+2}$ and $DV1_{71}{}^{+2}$ are responsible for n-type property of corresponding defective Si_xGe_{8-x}, which are shown in Fig. 7(b), (c) and (d), respectively. We then explain the influence of vacancy defects on the conductive properties of Si_1Ge_7 system as follows: For a Si SV defect in Si_1Ge_7 compound ($SV1_{17}$), there are four nearest atoms, each of which has one unpaired electron and results in one unsaturated covalent bond, as shown in Fig. 1. As a result, the $SV1_{17}{}^{+2}$ charged defect forms

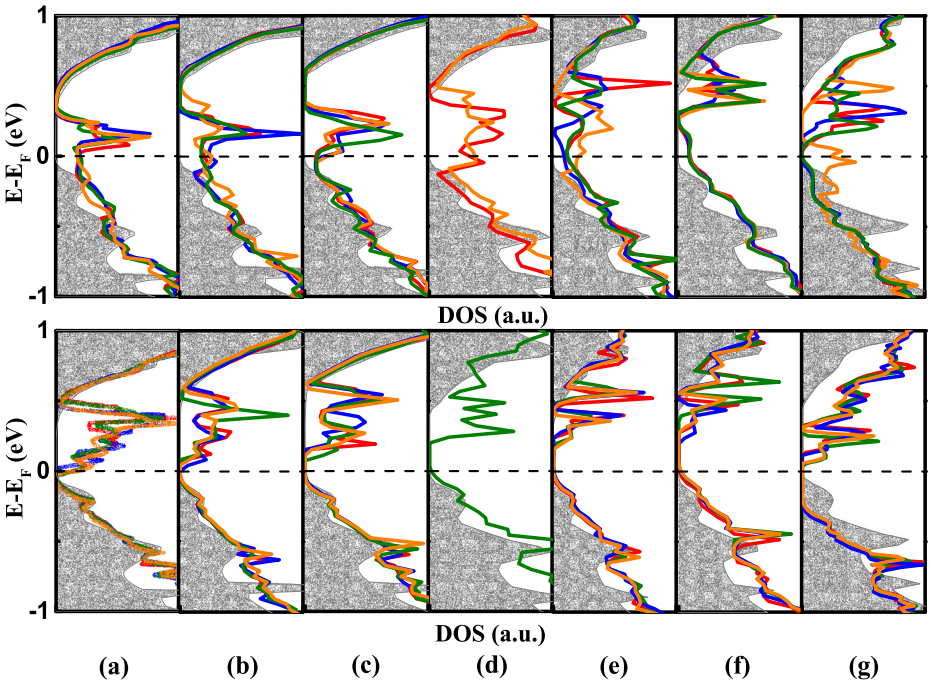

Fig. 6. (a)–(g) Density of state (DOS) for pristine and defective Si_xGe_{8-x} compounds Si_1Ge_7, Si_2Ge_6, …, Si_7Ge_1, respectively. The area under curve filled with gray color is denoted for the total DOS of pristine Si_xGe_{8-x} compounds, and colorized curves are for SV defects (upper) and DV defects (under) in their corresponding Si_xGe_{8-x} compounds.

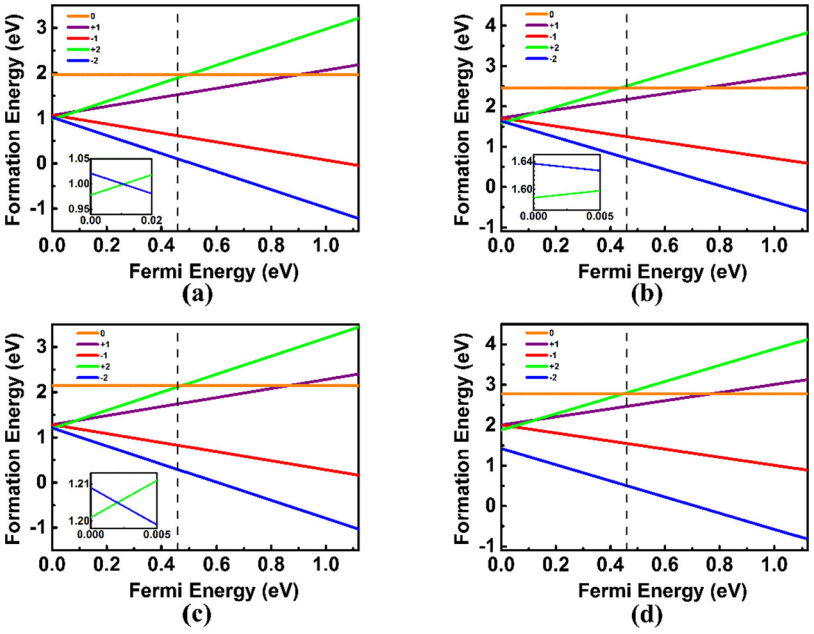

Fig. 7. Formation energies of the different charge states of the vacancy as a function of Fermi energy E_F. The zero of Fermi level corresponds to the top of the valence band, and the maximum corresponds to the energy gap of bulk Silicon (1.12 eV). The dash line is at the maximal E_g of Si_xGe_{8-x} (0.46 eV). (a) Formation energies of a Si vacancy ($SV1_{17}$) in Si_1Ge_7; (b) Formation energies of a double vacancy (one Si and one Ge atom lost) ($DV4_{17}$) in Si_1Ge_7; (c) Formation energies of a Si vacancy ($SV3_{71}$) in Si_7Ge_1; (d) Formation energies of a double vacancy (two Si atoms lost) ($DV1_{71}$) in Si_7Ge_1.

out and acts as an acceptor, leading to the trend of p-type band variation. For a DV defect in Si_1Ge_7 compound ($DV4_{17}$) as shown in Fig. 2, the surrounding nearest atoms leave further away from their original lattice positions owing to the bigger vacancy space. They behave like interstitial atoms, and their electrons could get lost since they don't form covalent bonds. As a result, the $DV4_{17}{}^{-2}$ charged defect forms out and acts as a donor, leading to the trend of n-type band variation. Besides, silicon atoms have smaller orbital radius, and the valence electrons are bounded more tightly, so they are more likely to act as an acceptor in defective Si_7Ge_1. Interestingly, we found that unintentionally doped $Si_{0.2}Ge_{0.8}$ single-crystalline samples grown on Ge substrate by ultra-high vacuum chemical vapor deposition [5] exhibit n-type property. Since two adjacent SV defects have a great possibility to coalesce a DV defect and result in n-type band as we found in this work, it is speculated that this n-type behavior of unintentionally doped SiGe samples should be caused by some kinds of DVs or related defects.

4. Conclusions

In this paper, we performed DFT calculations to investigate the influences of vacancy defects on the conductive properties of Si_xGe_{8-x} compounds. The study of formation energies of the defects indicates that a Si atom is easier to lose than a Ge to form a SV defect in Si_xGe_{8-x}, and DV defects might be more frequently found than two adjacent SV defects in SiGe. Most of the defective Si_xGe_{8-x} compounds with SVs show a trend to become to p-type, and almost all of the defective Si_xGe_{8-x} compounds with DVs turn to n-type. Vacancies with $+2$ charged state act as an acceptor, leading to the trend of p-type band variation, while -2 charged state act as a donor, leading to the trend of n-type band variation. Our work may provide insights into the future design and fabrication of conductive SiGe materials and devices.

CRediT authorship contribution statement

Limeng Shen: Data curation, Methodology, Software, Writing - Original draft preparation. **Xi Zhang:** Supervision, Writing - Reviewing and Editing. **Jiating Lu:** Software, Investigation. **Jiaqi Wang:** Validation. **Cheng Li:** Visualization, Investigation. **Gang Xiang:** Conceptualization, Supervision, Writing - Reviewing and Editing.

Declaration of competing interest

The authors have no affiliation with any organization with a direct or indirect financial interest in the subject matter discussed in the manuscript, and no known competing financial interests or personal relationships that could have appeared to influence the work reported in this paper.

Acknowledgements

This work was supported by National Key R&D Plan of China through Grant No. 2017YFB0405702 and National Natural Science Foundation of China through Grant No. 51672179.

Appendix A. Supplementary material

Supplementary material related to this article can be found online at https://doi.org/10.1016/j.physleta.2020.126993.

References

[1] D. Rideau, M. Feraille, L. Ciampolini, M. Minondo, C. Tavernier, H. Jaouen, A. Ghetti, Strained Si, Ge, and $Si_{1-x}Ge_x$ alloys modeled with a first-principles-optimized full-zone $k \cdot p$ method, Phys. Rev. B, Condens. Matter Mater. Phys. 74 (2006) 1–20, https://doi.org/10.1103/PhysRevB.74.195208.

[2] K. Moriguchi, S. Munetoh, A. Shintani, First-principles study of $Si_{34-x}Ge_x$ clathrates: direct wide-gap semiconductors in Si-Ge alloys, Phys. Rev. B 62 (2000) 7138–7143, https://doi.org/10.1103/PhysRevB.62.7138.

[3] J.F. Nützel, C.M. Engelhardt, R. Wiesner, D. Többen, M. Holzmann, G. Abstreiter, Growth and properties of high-mobility two-dimensional hole gases in Ge on relaxed Si/SiGe, Ge/SiGe buffers and Ge substrates, J. Cryst. Growth 150 (1995) 1011–1014, https://doi.org/10.1016/0022-0248(95)80092-Q.

[4] T. Tanaka, Y. Hoshi, K. Sawano, Y. Shiraki, K.M. Itoh, Upper limit of two-dimensional hole gas mobility in Ge/SiGe heterostructures, in: 2012 Int. Silicon-Germanium Technol. Device Meet. ISTDM 2012 - Proc. 222102, 2012, pp. 40–41.

[5] J. Wang, L. Shen, G. Lin, J. Wang, J. Xu, S. Chen, G. Xiang, C. Li, Homoepitaxy of Ge on ozone-treated Ge(1 0 0) substrate by ultra-high vacuum chemical vapor deposition, J. Cryst. Growth 507 (2019) 113–117, https://doi.org/10.1016/j.jcrysgro.2018.11.003.

[6] Z. Cheng, M.T. Currie, C.W. Leitz, G. Taraschi, E.A. Fitzgerald, J.L. Hoyt, D.A. Antoniadas, S. Member, S. Ge, Electron mobility enhancement in strained-Si substrates, IEEE Electron Device Lett. 22 (2001) 321–323.

[7] M.L. Lee, E.A. Fitzgerald, M.T. Bulsara, M.T. Currie, A. Lochtefeld, Strained Si, SiGe, and Ge channels for high-mobility metal-oxide-semiconductor field-effect transistors, J. Appl. Phys. 97 (2005) 1–27, https://doi.org/10.1063/1.1819976.

[8] C. Li, Q. Yang, H. Wang, J. Zhu, L. Luo, J. Yu, Q. Wang, Y. Li, J. Zhou, C. Lin, $Si_{1-x}Ge_x$/Si resonant-cavity-enhanced photodetectors with a silicon-on-oxide reflector operating near 1.3 μm, Appl. Phys. Lett. 77 (2000) 157–159, https://doi.org/10.1063/1.126909.

[9] B. Zhang, T. Zheng, Q. Wang, Z. Guo, M.J. Kim, H.N. Alshareef, B.E. Gnade, Stable and low contact resistance electrical contacts for high temperature SiGe thermoelectric generators, Scr. Mater. 152 (2018) 36–39, https://doi.org/10.1016/j.scriptamat.2018.03.040.

[10] M. Myronov, D.R. Leadley, Y. Shiraki, High mobility holes in a strained Ge quantum well grown on a thin and relaxed $Si_{0.4}Ge_{0.6}$/LT-$Si_{0.4}Ge_{0.6}$/Si(001) virtual substrate, Appl. Phys. Lett. 94 (2009) 2–5, https://doi.org/10.1063/1.3090034.

[11] E. Murakami, K. Nakagawa, A. Nishida, M. Miyao, Strain-controlled Si–Ge modulation-doped FET with ultrahigh hole mobility, IEEE Electron Device Lett. 12 (1991) 71–73, https://doi.org/10.1109/55.75707.

[12] G. Lin, X. Lan, N. Chen, C. Li, D. Huang, S. Chen, W. Huang, J. Xu, H. Lai, Strain evolution of SiGe-on-insulator fabricated by germanium condensation method with over-oxidation, Mater. Sci. Semicond. Process. 56 (2016) 282–286, https://doi.org/10.1016/j.mssp.2016.09.003.

[13] Y. Bogumilowicz, J.M. Hartmann, F. Laugier, G. Rolland, T. Billon, N. Cherkashin, A. Claverie, High germanium content SiGe virtual substrates grown at high temperatures, J. Cryst. Growth 283 (2005) 346–355, https://doi.org/10.1016/j.jcrysgro.2005.06.036.

[14] S. Marchionna, A. Virtuani, M. Acciarri, G. Isella, H. von Kaenel, Defect imaging of SiGe strain relaxed buffers grown by LEPECVD, Mater. Sci. Semicond. Process. 9 (2006) 802–805, https://doi.org/10.1016/j.mssp.2006.09.003.

[15] L. Fedina, O. Lebedev, G. Van Tendeloo, J. Van Landuyt, O. Mironov, E. Parker, In situ HREM irradiation study of point-defect clustering in MBE-grown strained structures, Phys. Rev. B, Condens. Matter Mater. Phys. 61 (2000) 10336–10345, https://doi.org/10.1103/PhysRevB.61.10336.

[16] H.M. Manasevit, I.S. Gergis, A.B. Jones, Electron mobility enhancement in epitaxial multilayer Si-$Si_{1-x}Ge_x$ alloy films on (100) Si, Appl. Phys. Lett. 41 (1982) 464–466, https://doi.org/10.1063/1.93533.

[17] T. Ohba, S.I. Ikawa, Far-infrared absorption of silicon crystals, J. Appl. Phys. 64 (1988) 4141–4143, https://doi.org/10.1063/1.341325.

[18] B. Rau, I. Sieber, B. Selle, S. Brehme, U. Knipper, S. Gall, W. Fuhs, Homoepitaxial Si absorber layers grown by low-temperature ECRCVD, Thin Solid Films 451–452 (2004) 644–648, https://doi.org/10.1016/j.tsf.2003.11.058.

[19] P.D. Wang, Summary abstract: growth of n-type Ge on Si by MBE, J. Vac. Sci. Technol., B Microelectron. Nanometer Struct. 2 (1984) 209, https://doi.org/10.1116/1.582783.

[20] M. Miyao, K. Toko, T. Tanaka, T. Sadoh, High-quality single-crystal Ge stripes on quartz substrate by rapid-melting-growth, Appl. Phys. Lett. 95 (2009) 1–4, https://doi.org/10.1063/1.3182795.

[21] T.F. Kuech, M. Mäenpää, S.S. Lau, Epitaxial growth of Ge on ⟨100⟩ Si by a simple chemical vapor deposition technique, Appl. Phys. Lett. 39 (1981) 245–247, https://doi.org/10.1063/1.92695.

[22] L. Wei, Y. Miao, Y.-F. Ding, C. Li, H. Lu, Y.-F. Chen, Ultra high hole mobility in Ge films grown directly on Si(100) through interface modulation, J. Cryst. Growth (2020) 125838, https://doi.org/10.1016/j.jcrysgro.2020.125838.

[23] I. Yonenaga, W.J. Li, T. Akashi, T. Ayuzawa, T. Goto, Temperature dependence of electron and hole mobilities in heavily impurity-doped SiGe single crystals, J. Appl. Phys. 98 (2005), https://doi.org/10.1063/1.2035890.

[24] I. Yonenaga, T. Akashi, T. Goto, Thermal and electrical properties of Czochralski grown GeSi single crystals, J. Phys. Chem. Solids 62 (2001) 1313–1317, https://doi.org/10.1016/S0022-3697(01)00026-9.

[25] D. Takahara, R. Yoshimine, T. Suemasu, K. Toko, High-hole mobility $Si_{1-x}Ge_x$ ($0.1 \leq x \leq 1$) on an insulator formed by advanced solid-phase crystallization, J. Alloys Compd. 766 (2018) 417–420, https://doi.org/10.1016/j.jallcom.2018.06.357.

[26] Y. Kim, M. Yokoyama, N. Taoka, M. Takenaka, S. Takagi, Ge-rich SiGe-on-insulator for waveguide optical modulator application fabricated by Ge condensation and SiGe regrowth, Opt. Express 21 (2013) 19615, https://doi.org/10.1364/oe.21.019615.

[27] N.V. Morozova, I.V. Korobeinikov, N.V. Abrosimov, S.V. Ovsyannikov, Controlling the thermoelectric power of silicon-germanium alloys in different crystalline phases by applying high pressure, CrystEngComm 22 (2020), https://doi.org/10.1039/d0ce00672f.

[28] L. Shen, M. Lan, X. Zhang, G. Xiang, The structures and diffusion behaviors of point defects and their influences on the electronic properties of 2D stanene, RSC Adv. 7 (2017) 9840–9846, https://doi.org/10.1039/c6ra28155a.

[29] M. Sun, J.P. Chou, A. Hu, U. Schwingenschlögl, Point defects in blue phosphorene, Chem. Mater. 31 (2019) 8129–8135, https://doi.org/10.1021/acs.chemmater.9b02871.

[30] Y.J. Zheng, Y. Chen, Y.L. Huang, P.K. Gogoi, M.Y. Li, L.J. Li, P.E. Trevisanutto, Q. Wang, S.J. Pennycook, A.T.S. Wee, S.Y. Quek, Point defects and localized excitons in 2D WSe_2, ACS Nano 13 (2019) 6050–6059, https://doi.org/10.1021/acsnano.9b02316.

[31] J. Xiao, K. Yang, D. Guo, T. Shen, H.X. Deng, S.S. Li, J.W. Luo, S.H. Wei, Realistic dimension-independent approach for charged-defect calculations in semiconductors, Phys. Rev. B 101 (2020) 1–7, https://doi.org/10.1103/PhysRevB.101.165306.

[32] E.G. Seebauer, M.C. Kratzer, Charged point defects in semiconductors, Mater. Sci. Eng., R Rep. 55 (2006) 57–149, https://doi.org/10.1016/j.mser.2006.01.002.
[33] Y.N. Wu, X.G. Zhang, S.T. Pantelides, Fundamental resolution of difficulties in the theory of charged point defects in semiconductors, Phys. Rev. Lett. 119 (2017) 1–6, https://doi.org/10.1103/PhysRevLett.119.105501.
[34] P. Deák, Q. Duy Ho, F. Seemann, B. Aradi, M. Lorke, T. Frauenheim, Choosing the correct hybrid for defect calculations: a case study on intrinsic carrier trapping in β-Ga_2O_3, Phys. Rev. B 95 (2017) 1–11, https://doi.org/10.1103/PhysRevB.95.075208.
[35] G. Kresse, J. Furthmüller, Efficiency of ab-initio total energy calculations for metals and semiconductors using a plane-wave basis set, Comput. Mater. Sci. 6 (1996) 15–50, https://doi.org/10.1016/0927-0256(96)00008-0.
[36] P.E. Blöchl, Projector augmented-wave method, Phys. Rev. B 50 (1994) 17953–17979, https://doi.org/10.1103/PhysRevB.50.17953.
[37] J.P. Perdew, K. Burke, M. Ernzerhof, Generalized gradient approximation made simple, Phys. Rev. Lett. 77 (1996) 3865–3868, https://doi.org/10.1103/PhysRevLett.77.3865.
[38] D. Wang, D. Han, X. Bin Li, N.K. Chen, D. West, V. Meunier, S. Zhang, H.B. Sun, Charged defects in two-dimensional semiconductors of arbitrary thickness and geometry: formulation and application to few-layer black phosphorus, Phys. Rev. B 96 (2017) 1–7, https://doi.org/10.1103/PhysRevB.96.155424.
[39] G.L. Pearson, J. Bardeen, Electrical properties of pure silicon and silicon alloys containing boron and phosphorus, Phys. Rev. 75 (1949) 865–883, https://doi.org/10.1103/PhysRev.75.865.
[40] W.R. Thurber, Resistivity-dopant density relationship for phosphorus-doped silicon, J. Electrochem. Soc. 127 (1980) 1807, https://doi.org/10.1149/1.2130006.
[41] J. Vanhellemont, O. De Gryse, S. Hens, P. Vanmeerbeek, D. Poelman, P. Clauws, E. Simoen, C. Claeys, I. Romandic, A. Theuwis, G. Raskin, H. Vercammen, P. Mijlemans, Grown-in lattice defects and diffusion in Czochralski-grown germanium, Defect Diffus. Forum 230–232 (2004) 149–176, https://doi.org/10.4028/www.scientific.net/ddf.230-232.149.
[42] T. Sinno, E. Dornberger, W. Von Ammon, R.A. Brown, F. Dupret, Defect engineering of Czochralski single-crystal silicon, Mater. Sci. Eng., R Rep. 28 (2000) 149–198, https://doi.org/10.1016/S0927-796X(00)00015-2.
[43] J. Vanhellemont, P. Spiewak, K. Sueoka, I. Romandic, On intrinsic point defect cluster formation during Czochralski crystal growth, Phys. Status Solidi Curr. Top. Solid State Phys. 6 (2009) 1906–1911, https://doi.org/10.1002/pssc.200881456.
[44] M.S. Hybertsen, S.G. Louie, Electron correlation in semiconductors and insulators: band gaps and quasiparticle energies, Phys. Rev. B 34 (1986) 5390–5413, https://doi.org/10.1103/PhysRevB.34.5390.
[45] R.E. Mapasha, M.P. Molepo, R.C. Andrew, N. Chetty, Defect charge states in Si doped hexagonal boron-nitride monolayer, J. Phys. Condens. Matter 28 (2016), https://doi.org/10.1088/0953-8984/28/5/055501.
[46] A.V. Krukau, O.A. Vydrov, A.F. Izmaylov, G.E. Scuseria, Influence of the exchange screening parameter on the performance of screened hybrid functionals, J. Chem. Phys. 125 (2006), https://doi.org/10.1063/1.2404663.
[47] F. Corsetti, A.A. Mostofi, System-size convergence of point defect properties: the case of the silicon vacancy, Phys. Rev. B, Condens. Matter Mater. Phys. 84 (2011) 1–9, https://doi.org/10.1103/PhysRevB.84.035209.